www.cadanda.com
Computer-Aided Design AND APPLICATIONS

An Analysis of the Elliptical Cup Hydraulic Drawing Process

Yuung-Ming Huang[1]

[1]St. John's University, hyming@mail.sju.edu.tw

ABSTRACT

In this study, finite element was utilized to simulate elliptical cup hydroforming deep drawing to explore the relationship between the punch load and stroke, workpiece thickness changes, the major stress distribution, the punch fillet radius, hydrostatic pressure, deformation mechanism and the forming limit, etc., in the process of forming. The numerical simulation and experimental results show that the punch load increases as the stroke increases and levels off until the forming is done. The maximum punch load and punch fillet radius is proportional. When the hydraulic pressure grows larger, the bottom of the cup and the fillet become thinner; the maximum punch load value is also increased due to increased hydraulic pressure. The minimum thickness value is concentrated in the junction of the workpiece and long axis of the punch. And due to a larger radius of curvature, the short axis region bears smaller circumferential tensile stress; therefore, there is little change in thickness. The limit drawing ratio (LDR) as defined by elliptical punch perimeter and the original sheet perimeter shows that the limit drawing ratio for an elliptical cup hydroforming deep drawing is 2.056.

Keywords: finite element, hydroforming deep drawing, limit drawing ratio.
DOI: 10.3722/cadaps.2012.375-383

1 . INTRODUCTION

The drawing is a forming method usually applied to the metal shell barrel-shaped vessel product, for example, the shells each for the battery of 3C electronic industry, micro motor, bullet, and fender of auto-body stamping. In a traditional drawing, the friction on the wall of the product upon forming will adversely affect the forming of the product rendering that a larger limit drawing ratio (LDR) cannot be achieved. During the drawing forming, associated with hydraulic pressure and hydraulic device, the sheet is made into shape under the effect of close leaning to punch, which is the so-called hydroforming deep drawing. In this study, the hydraulic pressure drawing of sheet metal forming is used in which the product is immersed into the hydraulic pressure oil to allow the product evenly bear the pressure so as to promote the strength of the product and to achieve a better surface of the product meanwhile the friction on the wall during forming will be reduced to achieve a very high LDR so as to reduce the drawing cycles and save the cost.

As the strain hardening exponent n value and the anisotropy index r value of the aluminum-magnesium alloy and other light metal materials are small, the drawing performance is poorer; so, the

use of hydroforming deep drawing can improve the forming limit of this type, of low plasticity, and hard-to-shape, material and reduce the processing pass of forming [1-3]. Lang [4-5] and others with finite element simulation and experiment pointed out that the value of the hydraulic pressure will affect the wall thickness of sheet metal after forming, and tried to find out the processing pressure for making uniform thickness and the curve of the punch mechanism and explore the hydraulic forming properties and damage limit of the anisotropic materials (AL6016-T4).

Zaky [6] and others with low carbon steel and industrial aluminum sheet, to carry out elliptical cup hydroforming deep drawing experiments, aimed at making the most ideal shape under the precondition that the material would not produce the protruding ear. Hah [7] and others chose shell element to implement finite element analysis, and then modified the sheet metal in order to get the consistency between simulation and experimental results. Experimental results show that localized deformation occurs along the long axis, and wrinkling is most likely formed on the short axis. The main reasons are inconsistent drawing rates of the long and short axes and positioning problem between dies in the process of forming. Kim [8] and others proposed bifurcation theory to carry out the finite element analysis of elliptical cup hydroforming deep drawing. In the text the long axis was fixed at 80 mm, and the short axis, as variables, at 40 mm as initial size and increased by 10 mm after each experiment. The experiments showed when the short axis was 60 mm (aspect ratio of 1.333), the first wrinkle occurred, and with the increase of aspect ratio of punch the wrinkles formation tended to level off. Near the area around the long axis the phenomenon of rupture occurred in advance.
This study conducts the simulation and experiments of hydroforming deep drawing on sheet metal of different initial outer diameters by elliptical punch, and explores and compares their results, such as the relationship between the punch load and stroke, the distribution of the equivalent strain, thickness distribution and forming limit, etc., of the workpiece.

2. BASIC THEORY

The equation for virtual work can be made discrete. The updated Lagrangian formulation (ULF) in a framework of the application of an incremental deformation for the metal forming process can be practically applied to describe the incremental properties of plastic flow. The current configuration according to ULF at each stage of deformation is used as a reference state to evaluate the deformation during a small time interval Δt, such that first-order theory is consistent with the required accuracy.

The rate equation for virtual work written as an updated Lagrangian equation is

$$\int_V \left(\tilde{\tau}_{ij} - 2\sigma_{ik}\dot{\varepsilon}_{kl}\right)\delta\dot{\varepsilon}_{ij}dV + \int_V \sigma_{ik}L_{ik}\delta L_{ij}dV = \int_{S_f} \dot{\bar{t}}_i \delta v_i dS \tag{1}$$

where V and S_f are the material volumes and the surface on which the traction is prescribed. $\tilde{\tau}_{ij}$ is the Jaumann rate of Cauchy stress, σ_{ij} is the Cauchy stress, $\dot{\varepsilon}_{kl}$ the rate of deformation, which is the symmetric part of the velocity gradient $L_{ik}\left(=\partial v_i/\partial X_j\right)$, in which v_i is the velocity, and $\dot{\bar{t}}_i$ is the rate of the nominal traction.

As the principle of virtual work rate equation and the constitutive relation are linear equations of rates, these can be replaced by increments defined with respect to any continuously increasing measure, such as the tool displacement increment.

Applying the standard procedure of finite elements to form the complete global stiffness matrix, yields

$$[K]\{\Delta u\} = \{\Delta F\} \tag{2}$$

in which

$$[K] = \sum_{\langle e\rangle}\int_{V\langle e\rangle}[B]^T\left(\left[D^{ep}\right]-[Q]\right)[B]dV + \sum_{\langle e\rangle}\int_{V\langle e\rangle}[E]^T[G][E]dV \tag{3}$$

$$\{\Delta F\} = \left(\sum_{S\langle e\rangle}[N]^T\left\{\dot{\bar{t}}\right\}dS\right)\Delta t \tag{4}$$

Capacity	130 ton
upper pressure (inner) capacity	80 ton
lower pressure (outer) capacity	50 ton
the lower table area	400 mm * 500 mm
upper plate stroke	350 mm
he maximum counter hydraulic pressure	70 MPa (700 bar)
ejection capacity	50 ton

Tab. 1: The equipment specifications of Sheet Metal Counter Hydraulic Forming Machine.

In these equations, $[K]$ is the global tangent matrix, $[D^{ep}]$ is the elemental elasto-plastic constitutive matrix, $[N]$ is the shape function matrix, $[B]$ is the strain rate-velocity matrix, $[E]$ is the velocity gradient-velocity matrix, $\{\Delta u\}$ denotes the nodal displacement increment, and $\{\Delta F\}$ denotes the prescribed nodal force increment. $[Q]$ and $[G]$ are defined as stress correction matrices due to the current stress states at any stage of deformation.

In view of contact or separation between the sheet metal and die during the Elliptical cup hydroforming deep drawing process, appropriate boundary conditions must be set up depending on the contact condition of the sheet metal with the die for numerical analysis. When forming is finished, the springback is a crucial factor in sheet metal forming. After removal of load, the sheet metal will rebound to an ultimate size of stress equilibrium which is the final size. When the dies are completely removed, the rebound counting begins. The boundary conditions of the new force are specified at all contact nodes and set as $\Delta f = -f$.

3. EXPERIMENTALAND NUMERICAL ANALYSIS

3.1. Experimental Equipment and Methods

Experimental equipment of this study includes a sheet metal counter hydraulic forming machine of 130 tons and a set of data capture equipment. Equipment and specifications are as shown in Fig. 1 and Table 1.Die components include an elliptical punch, dies and the holder. The length of the axis of punch are 60 mm and 38 mm respectively, and punch and die radius are $R_P = 5$ mm and $R_D = 5$ mm respectively, as shown in Fig. 2 and Fig. 3.The hydrostatic pressure is $P = 25$ MPa , and the punch speed is 1000 mm/s. The main role of hydraulic chamber pressure is on the one hand to increase the useful friction between the sheet metal and the punch to stop the continual thinning of the sheet metal in the region that forming has been achieved. On the other hand, it establishes the fluid lubrication between the sheet metal and the punch to reduce the frictional force caused by binder force; thus, the increasing scale of radial tensile stress is eased.

3.2. Finite element simulation

A commercial software package I-DEAS is used for pre-processing, the established die and sheet metal segregated through the grid, and conversion made to conduct numerical analysis of the processes of the elliptical cup hydroforming deep drawing. Analysis of the friction between sheet metal and die is done using the Coulomb's law, Die mesh segmentation uses triangular element, and sheet metal mesh segmentation uses Quadrilateral four-node shell element (Belytschko-Tsay), which is suitable for nonlinear material models and widely used in the forming problems of large deformation and large rotation. The entire model uses ULF (update Lagrangian Formulation) as reference coordinates for processing; the solution criteria in the forming analysis use Full Newton-Raphson iteration solution; and the convergence criteria use the Relative residual displacement. The analytical

Fig. 1:Sheet Metal Counter Hydraulic Forming Machine.

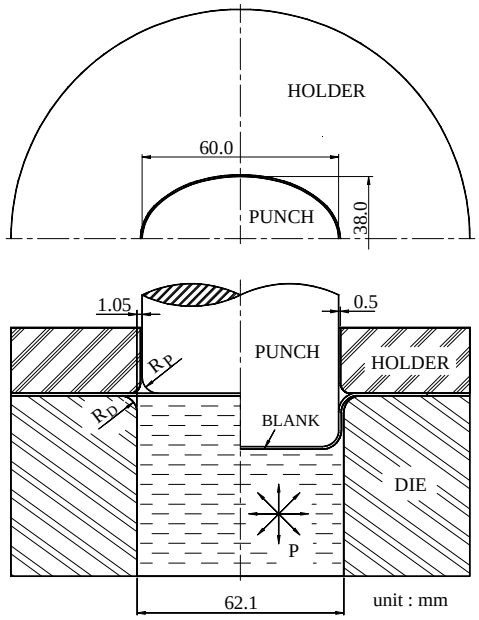

Fig. 2: Geometric size of elliptical cup hydroforming deep drawing die.

Holder Punch Die

Fig. 3: The tools of elliptical cup drawing forming.

convergence error is $\frac{\|\delta_u\|_{\max}}{\|\Delta_u\|_{\max}} < 0.1\%$, in which the $\|\Delta_u\|$ is the amount of change in displacement increment, and $\|\delta_u\|$ is the amount of displacement change in iteration solution.

3.3. Material Parameters

The material is CA-CQ1F (SPCC) which is made by the continuous annealing process and is sheet metal having the carbon content of 0.03-0.06. The material data for sheet steel, supplied by the China Steel Corporation, was tested according to ASTM E646-78 in the directions of 0°, 45°, and 90° with respect to the rolling direction for calculation and experiment. The material used to manufacture the die is JIS G4404 SKD11. The tensile sheet specimens underwent standard tensile testing under continuous loading to failure. The least-square method was applied to approximate the true stress-strain relationship as a power law for work-hardening. The material data are as follows:

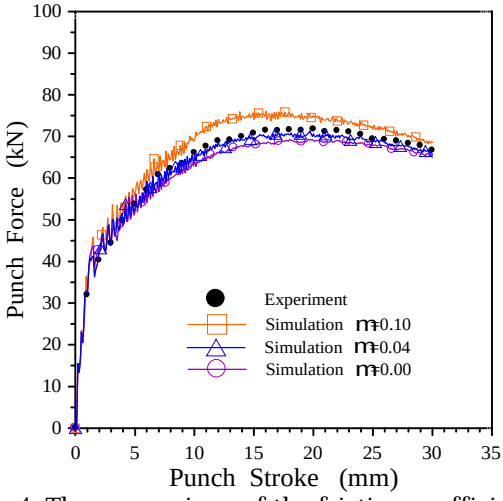

Fig. 4: The comparison of the friction coefficient to the punch load distribution.

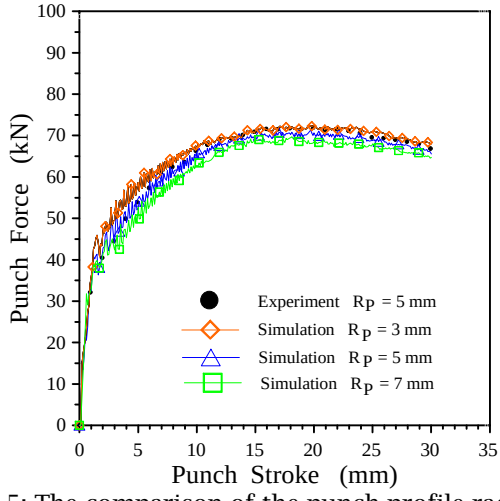

Fig. 5: The comparison of the punch profile radius to the punch load distribution.

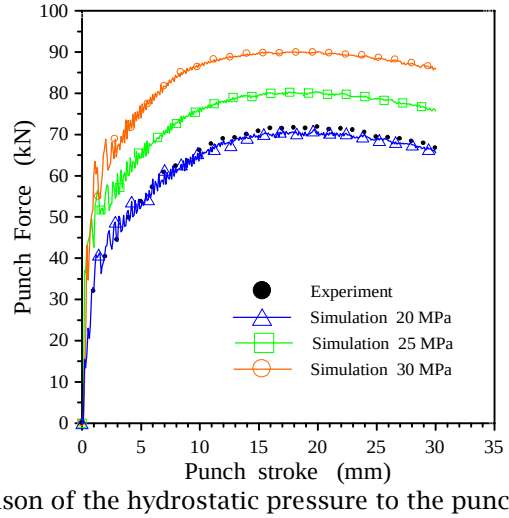

Fig. 6: The comparison of the hydrostatic pressure to the punch load distribution.

- thickness: $t = 0.8$ mm
- yield stress: $\sigma_y = 279$ MPa
- fracture thickness in the simple tensile test: $t_f = 0.645$ mm
- stress-strain : $\bar{\sigma} = 580.6\left(0.01291 + \bar{\varepsilon}^p\right)^{0.286}$
- Poisson's ratio : $\upsilon = 0.30$
- Young's modulus: $E = 2.1\times10^5$ MPa
- averaged planar anisotropy : $\bar{r} = 1.10$

4. RESULTSANDDISCUSSION

4.1. Comparison of Forming Load

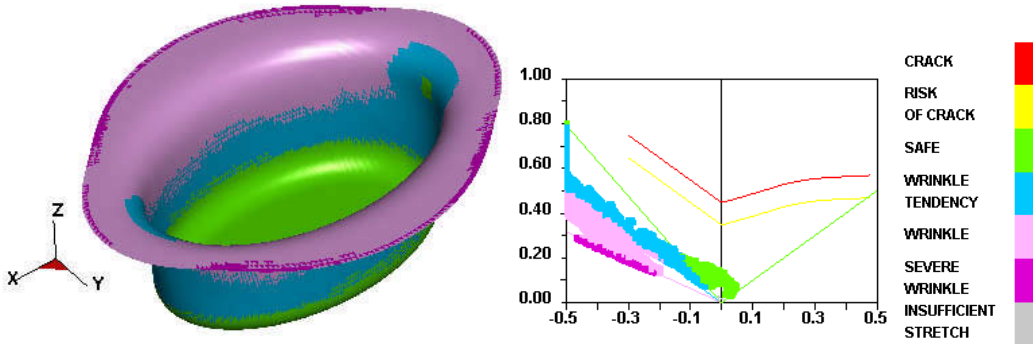

Fig. 7: The simulated deformation and forming diagram (sheet metal diameter 102mm).

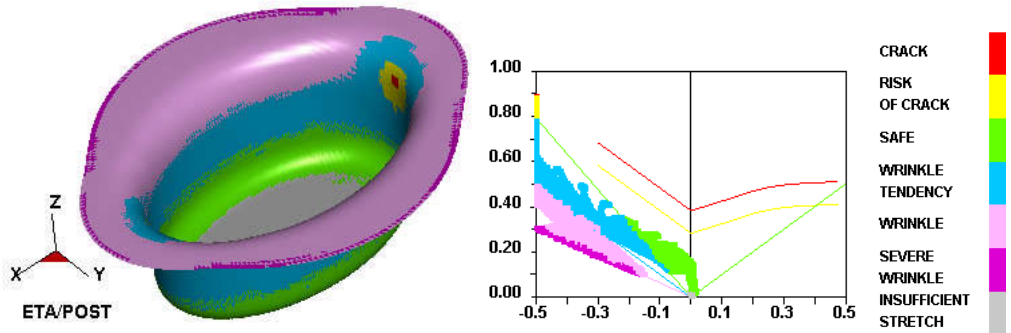

Fig. 8:The simulated deformation and forming diagram (sheet metal diameter 103mm).

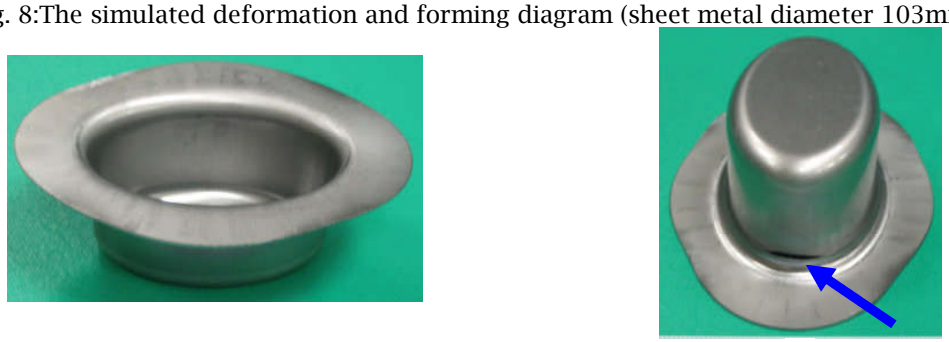

(a) (b)

Fig. 9: The experimental product of elliptical cup hydroforming deep drawing (a) sheet metal diameter 10mm;(b) sheet metal diameter 103mm (observe the crack).

From Fig. 4 we can see that the punch load increases as the stroke increases until the stroke reaches 16.5 mm. The punch load then reaches the maximum value, the sheet metal continues the deformation along with the increase of the stroke, and the load is dropped. The larger the friction coefficient is, the larger the value of its load will be. When the friction coefficient is $\mu = 0.04$, the simulated load is more consistent with the experiments; therefore, this study used the simulation results of $\mu = 0.04$ to compare with the experimental results.

The total drawing load consists of the ideal forming load and an additional component to compensate for friction in the contacting areas of the flange region and bending forces at the die radius. The forming load is transferred from the punch radius through the drawn part wall into the deformation region. Fig. 5 shows the relations of the compressive load and punch stroke with different punch fillet radii. Experiments applied the press oil lubricant while the simulation used a friction coefficient $\mu = 0.04$, and the results obtained were consistent. In the drawing process of punch stroke, the punch load is in inverse proportion to the punch fillet radii.

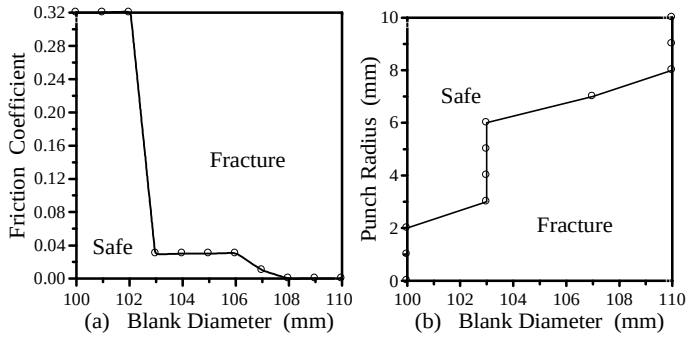

Fig. 10: The impact of the friction coefficient, punch shoulder radius and sheet metal diameter in the forming.

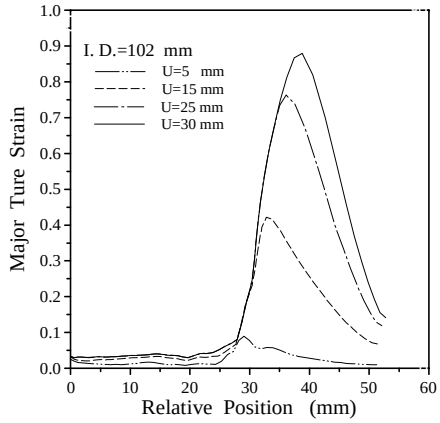

Fig. 11: Distribution of the long axis major strain.

Based on Fig. 5, in the initial stage of punch stroke, the punch load is in inverse proportion to the punch profile radius. With increasing the punch stroke, the sheet metal which has a larger punch profile radius, upon the function of hydraulic pressure, will have a larger punch touching area and a longer punch stroke corresponding to the occurrence of loading peak value. That is contrary to the results achieved from the traditional drawing. From Fig. 6 we can see that punch load increases as the hydraulic pressure increases.

4.2. Deformation and Forming Limit Diagram

Forming limit used to measure the fracture resistance of sheet metal is the most important indicator in forming. Its size is mainly restricted by plastic instability (rupture and wrinkling) and generally can be expressed by maximum deformation bearable extent before the instability of the sheet metal occurs. This article also defined the drawing ratio (DR), limit drawing ratio (LDR) and excessive drawing ratio (EDR), as indicated below:

$$\mathrm{DR} = C_h / C_p \tag{5}$$

$$\mathrm{LDR} = C_{h,\min} / C_p \tag{6}$$

$$\mathrm{EDR} = C_{h,f} / C_p \tag{7}$$

In the formulation, C_p stands for perimeter of elliptical punch, C_h for perimeter of the initial sheet metal where localized necking or rupture would not occur, $C_{h,\min}$ for perimeter of the minimum initial sheet metal where localized necking or rupture would not occur, and $C_{h,f}$ for perimeter of initial sheet metal where localized necking or rupture will occur. When the sheet metal is 102 mm in diameter (LDR = 2.056), no phenomenon of necking or rupture occurs in the direction of the long axis or the short

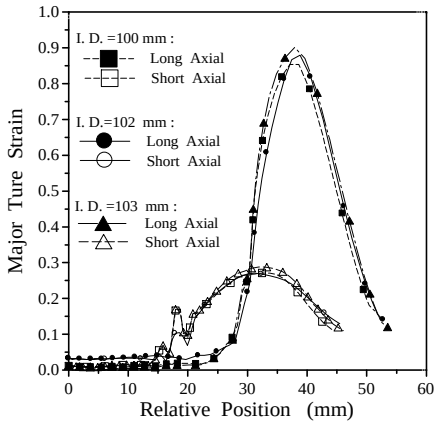

Fig. 12: Distribution of the long and short axis major strain.

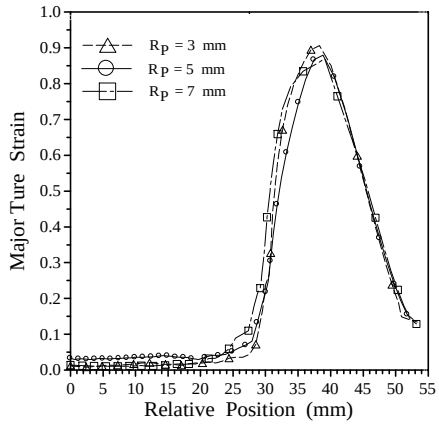

Fig. 13: Relationship between punch fillet radius and the long axis major strain.

axis, as shown in Fig. 7.When the sheet metal is 103 mm in diameter (EDR = 2.076), due to the effect of hydrostatic pressure, the part formed does not carry on with drawing forming under the action of useful friction but continues in the deformation. However, the harmful friction between the sheet metal and binder board increases under the action of hydraulic pressure at the convex edge areas of the sheet metal along the direction of long axis. At the same time, the increased thickness of sheet metal also increases the friction with the die, leading to excessive radial drawing stress at the punch die shoulder fillet along the long axis of sheet metal. The rupture occurs near the punch die shoulder fillet in the latter stage along the long axis, as shown in Fig. 8.The simulated deformation and the forming limit diagram in Fig. 7 and Fig. 8 can be confirmed by the experiments of Fig.9.

4.3. The Effect of Processing Parameters

Fig.10(a) shows that when the diameter of sheet metal is less than 102 mm or greater than 108 mm, the friction coefficient has no impact on the forming of sheet metal. But if the diameter is in between, then the smaller the friction coefficient is, the easier it is to shape. With increasing the punch radius, the forming of the sheet metal will be more mitigated and is more difficult to break. Even a blank which is with a larger diameter rendering its difficulty in forming is used, the forming of the sheet metal also will be more mitigated and is more difficult to break owing to the punch with a larger punch radius. On contrary, upon using the punch having a smaller punch radius, the forming of the sheet metal becomes difficult and thus a smaller radius punch shall be used to ensure the safety-forming. The relationship between the punch radius and the blank diameter is shown in Fig. 10(b). As the stroke increases, the major strain rises, and the maximum major strain position gradually deviates from the central axis and ends up in the die corner, as shown in Fig. 11. But because the geometric shape at the major axis is of a small radius of curvature, the circumferential stress to bear is larger. So, there is concentration phenomenon of higher stress. Therefore, the major strain of the long axis is much greater than that of short axis, as shown in Fig. 12. Because the larger sheet metal is not easy to shape, the major strain is also large. In the latter stage of forming, along the direction of long axis near the shoulder fillet of punch die, there is maximum major strain, and it is easy to cause forming rupture here. Using an elliptical cup of smaller punch fillet radius, the bottom has a smaller major strain, but it gradually increases along the fillet drawing to the direction of the side wall, as shown in Fig. 13.

5. CONCLUSION

This paper explores the analysis of the process of elliptical cup hydroforming deep drawing, such as the relationship between punch load and stroke, the distribution of major strain, the course of elliptical cup drawing forming and the forming limit, and so on. To design a set of a forming dies to

carry out an experiment of elliptical cup hydroforming deep drawing, and to obtain data required for forming by the data capture devices, the final is based on the results in comparison of the data obtained and the numerical analysis simulation, and the conclusion obtained is as follows:

1. Maximum punch load is proportional to punch fillet radius used, and along with the increase, the corresponding punch stroke when load peak occurs becomes longer.
2. The larger the friction coefficient and the hydraulic pressure are, the larger the corresponding punch loading is.
3. Forming workpiece variation in the distribution of major strain can be divided into three stages: at the first stage, due to the contact of punch with sheet metal, circumferential compressive stress and compressive strain were produced. In the direction of the long axis, tensile stress was formed. At the second stage, the sheet metal under the effect of the punch gradually formed straight walls of products. But the drawing forming was incomplete; therefore, there was circumferential tensile stress and even positive strain. At the third stage the workpiece had residual stress and compressive strain at the long axis, and there was stress concentration in the corner of the die shoulder.
4. The maximum strain value is concentrated in the region where the workpiece touches the long axis of the punch, because the sheet metal bears the maximum tensile stress at the long axis. The short axis region of the workpiece due to a larger curvature radius bears less circumferential tensile stress so that the variation of strain is more modest.

As defined by the perimeter of the elliptical cylinder punch and the perimeter of the initial sheet metal, the limit drawing ratio (LDR) of elliptical cup hydroforming drawing is 2.056.

REFERENCES

[1] Yu, Z.-Q.; Zhao, Y.-X.; Lin, Z.-Q.: Evaluation Parameter of Drawability of Automotive Aluminum Alloy Sheets, The Chinese Journal of Nonferrous Metals, 14(10), 2004, 1689-1693.

[2] Zhang, S.-H; Wang, Z.-R; Xu, Y.: Recent Developments in Sheet Hydroforming Technology, Journal of Materials Processing Technology, 151(1-3), 2004, 237-241.doi:10.1016/j.jmatprotec.2004.04.054

[3] Kang, D.-C.; Chen, Y.; Xu, Y.-C.: Hydromechanical Deep Drawing of Superalloy Cups, Journal of Materials Processing Technology, 166(2), 2005, 243-246. doi:10.1016/j.jmatprotec.2004.08.024

[4] Lang, L.; Danckert, J.; Nielsen, K.-B.: Study on Hydromechanical Deep Drawing with Uniform Pressure onto the Blank, International Journal of Machine Tools & Manufacture, 44(5), 2004, 495-502. doi:10.1016/j.ijmachtools.2003.10.028

[5] Lang, L.; Danckert, J.; Nielsen, K.-B.: Investigation into Hydrodynamic Deep Drawing Assisted by Radial Pressure Part II-Numerical Analysis of the Drawing Mechanism and the Process Parameters, Journal of Materials Processing Technology, 166(1), 2005, 150-161. doi:10.1016/j.jmatprotec.2004.08.015

[6] Zaky, A.-M.; Nassr, A.-B.; El-Sebaie, M.-G.: Optimum Blank Shape of Cylindrical Cups in Deep Drawing of Anisotropic Sheet Metals, Journal of Materials Processing Technology, 76(1-3), 1998, 203-211. doi:10.1016/S0924-0136(97)00349-X

[7] Has, H.; Kim, S.-H; Kim, S.-H.: Process Design for Multi-Stage Elliptic Cup Drawing with the Large Aspect ratio, European Congress on Computational Methods in Applied Sciences and Engineering, Barcelona:11-14 September, 2000.

[8] Kim, J.-B.; Yoon, J.-W.; Yang, D.-Y.; Barlat, F.: Investigation into Wrinkling Behavior in the Elliptical Cup Deep Drawing Process by Finite Element Analysis using Bifurcation-Theory, Journal of Materials Processing Technology, 111(1-3), 2001, 170-174. doi:10.1016/S0924-0136(01)00504-0.